Microbial Cell Factories

RESEARCH Open Access

Biocatalytic cascade for the synthesis of methylphosphonate from phosphoenolpyruvate

Qi Zhang[1], Yiming Zhang[2], Bobo Wang[1], Cong Wang[1], Renyuan Zhao[1] and Zhisheng Yu[1,3*]

Abstract

Background Methylphosphonate (Mpn), a building block for complex organophosphonate, is utilized in pharmaceuticals, agriculture, and chemical industries. It also serves as a critical substrate for resolving the methane paradox in ecological studies. However, current Mpn synthesis predominantly relies on chemical methods. Therefore, there is a growing interest in developing biosynthetic approaches for Mpn production.

Results In this study, the biosynthetic pathway of Mpn was reconstituted. Four crucial enzymes involved in the conversion of phosphoenolpyruvate (PEP) to Mpn were screened: phosphoenolpyruvate mutase (AepX), phosphonopyruvate decarboxylase (AepY), phosphonoacetaldehyde reductase (AlpJ), and methylphosphonate synthase (MpnS). Both in vitro and in vivo biocatalytic cascades were implemented. Through systematic optimization of the in vitro reaction conditions, a final Mpn conversion yield of 76% was achieved from 5 mM PEP, with an optimal enzyme concentration ratio of 5 μM AepX, 10 μM AepY, 10 μM AlpJ, and 10 μM MpnS. Building on the in vitro system, recombinant *Escherichia coli* strains co-expressing four enzymes were engineered as whole-cell catalysts. By employing a dual-plasmid system with varying copy numbers to regulate heterologous enzyme expression, engineered strains with distinct synthetic capabilities were obtained. The engineered strain E6 (harboring plasmids pCDFDuet-*aepX-aepY* and pETDuet-*alpJ-mpnS*) produced 7.19 mM Mpn, corresponding to a 35.95% molar conversion yield within 16 h.

Conclusions This study established a biosynthetic method for Mpn production from PEP through enzymatic cascade, operating under mild aqueous conditions.

Keywords Methylphosphonate, Phosphoenolpyruvate, Biocatalytic cascade, In vitro cascade, Enzymatic process optimization, Whole-cell catalysts

*Correspondence:
Zhisheng Yu
yuzs@ucas.ac.cn
[1]College of Resources and Environment, University of Chinese Academy of Sciences, No. 1 Yanqi Lake East Road, Huairou, Beijing 101408, China
[2]CAS Key Laboratory of Green Process and Engineering, Institute of Process Engineering, Chinese Academy of Sciences, Beijing 100190, P. R. China
[3]RCEES-IMCAS-UCAS Joint-Laboratory of Microbial Technology for Environmental Science, Beijing 100085, P. R. China

Background

Organophosphonates, characterized by their carbon-phosphorus (C-P) bond, exhibit exceptional stability and structural mimicry. These molecules not only exhibit bioactivities against microbes but also act as phosphorus sources under nutrient-limiting conditions. Methylphosphonate (Mpn), the simplest organophosphonate with a phosphonate group and a methyl group, exhibits diverse application potential. Mpn serves as a "building block" to create complex organophosphonates [1]. Predominantly, it is widely employed in chemical transformations [2], while its derivatives are integral to manufacturing pesticides, anticancer agents, antibiotics, and flame retardants [3, 4]. Notably, microbial catabolism of Mpn releases methane, which provides a plausible explanation for the "ocean methane paradox". Mpn can be used as a precursor substrate for methane production under aerobic conditions [5]. Therefore, Mpn plays a critical role in agriculture, chemical industry, pharmaceuticals, and ecology.

Currently, Mpn production primarily relies on chemical synthesis, such as the Michaelis-Arbuzov reaction (Fig. 1a), a common method for synthesizing organophosphonates with C-P bonds [6]. This reaction involves a trisubstituted phosphite as a nucleophile reacting with an alkyl halide at elevated temperature (135–150 °C) to replace the halogen. However, the generation of by-products can lower the reaction yield and cause environmental problems. Greener approaches have been developed for the Michaelis-Arbuzov reaction [7, 8]. For example, phosphonate can be efficiently generated in high yields (75–90%) using environmentally-benign alcohols instead of toxic alkyl halides in the presence of an iodide catalyst, with the main byproduct being an alcohol. The UV photolysis (185 nm) of acetone with phosphite can yield Mpn (Fig. 1b) at only 17% efficiency [1]. While some chemical methods have already achieved high yields [9, 10], there is a need for a gentler approach to Mpn production.

Biocatalysis has emerged as a cornerstone strategy in organic synthesis to accelerate chemical transformations with precision. These biocatalysts, primarily enzymes, leverage their exceptional substrate selectivity and operation under mild conditions to enable the synthesis of high-value chemicals, ranging from pharmaceuticals to agrochemicals [11]. Multi-enzyme cascades (also termed biocatalytic cascades) can be executed both in vitro and in vivo [12, 13]. In vitro cascade employs cell lysates or purified enzymes for substrate conversion, a strategy particularly advantageous for (i) reactions requiring non-physiological conditions (e.g., elevated temperatures), (ii) systems involving enzymes with low solubility, and (iii) processes where toxic intermediates necessitate spatial separation from host cells. Compared to metabolic engineering, this approach provides superior flexibility in enzyme dosage control and reaction order optimization. An outstanding example is the nine-enzyme in vitro

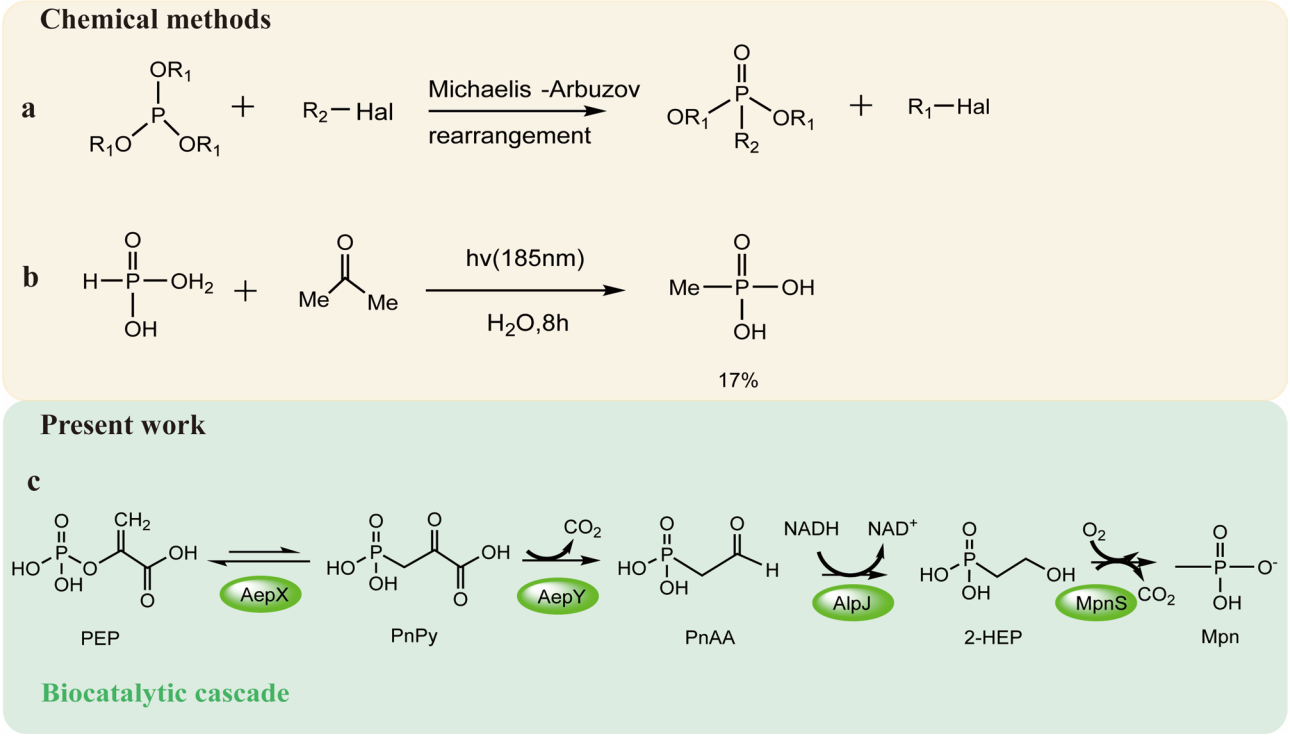

Fig. 1 Chemical and biocatalytic routes for Mpn production. **a** Michealis-Arbuzov reaction. **b** Simple UV photolysis reaction. **c** The biocatalytic cascade route

cascade that synthesizes islatravir, a promising anti-HIV drug candidate [14]. In vivo cascades, conversely, rely on the co-expression of heterologous enzymes within engineered microbial hosts (e.g., *Escherichia coli*) to create whole-cell biocatalysts [15]. The cell-wall could protect enzymes, improving substrate tolerance and operational stability [13]. For instance, azelaic acid, a critical monomer for biodegradable polymers, was efficiently produced via a three-enzyme in vivo cascade using linoleic acid as the substrate [16]. Therefore, biocatalytic cascades enables one-pot synthesis of target compounds with simple materials as substrates, which comply with the development of green chemistry [17, 18].

Metcalf et al. identified methylphosphonate synthase (MpnS) from the marine archaeon *Nitrosopumilus maritimus*, a breakthrough that unveiled the enzymatic basis of Mpn production [19]. Mechanistic studies revealed that MpnS catalyzed the oxidative cleavage of 2-hydroxyethylphosphonate (2-HEP) into Mpn and CO_2, thereby linking Mpn biosynthesis to methane release. Interestingly, various natural oraganophosphonates like fosfomycin [20], phosphinothricin tripeptide [21], and argolaphos [22] share a biosynthetic pathway involving the synthesis from PEP to 2-HEP, indicating a degree of pathway conservation [23]. Consequently, the identification of MpnS function has unveiled the complete Mpn biosynthetic pathway. The biosynthesis of phosphonate is initiated with C-P bond formation, a reaction catalyzed by PEP mutase. Thus, this gene is commonly utilized as a molecular marker for annotating phosphonate biosynthetic gene clusters [24]. Seidel et al. successfully cloned and overexpressed PEP mutase gene from *Tetrahymena pyriformis* in *E. coli*. They demonstrated PEP mutase role in catalyzing the conversion between PEP and phosphonopyruvate (PnPy) in equilibrium [25]. The equilibrium strongly favors PEP retention due to the high bond dissociation energy of the P-O bond in PEP (17–24 kcal/mol).

To the best of our knowledge, no prior study has reported the production of Mpn via enzymatic cascade reactions. This study aimed to reconstruct the Mpn biosynthetic pathway employing both in vitro and in vivo biocatalytic cascades. The cascade pathway consisted of four enzymatic reactions starting with phosphoenolpyruvate (PEP) as the substrate. Four enzymes with diverse functions, sourced from different microbial species, were systematically screened. The in vitro reaction conditions, including enzyme ratios, substrate and cofactor concentrations, were optimized. Building on in vitro system, an in vivo cascade system was further developed to facilitate simplified Mpn biosynthesis. Recombinant *E. coli* strains were engineered to co-expressing four enzymes as whole-cell catalysts. A dual-plasmid expression system was utilized to precisely regulate intracellular enzyme levels.

Results

Pathway and enzyme selection

By searching the Kyoto Encyclopedia of Genes and Genomes (KEGG) database for MpnS enzyme, we located the complete biosynthetic pathway of Mpn within the phosphonate metabolism pathway (KEGG map 00440). PEP, a central metabolic intermediate, was chosen as the starting substrate. A four-step enzymatic cascade was selected containing rearrangement, decarboxylation, reduction, and oxidation (Fig. 1c). This pathway involves sequential enzymatic transformations. The initial reaction was catalyzed by PEP mutase, which converted PEP into PnPy. Subsequently, phosphonopyruvate decarboxylase decarboxylated PnPy to generate phosphonoacetaldehyde (PnAA). This reaction required thiamine diphosphate (TPP) and Mg^{2+} as essential cofactors. The resulting PnAA was then reduced to 2-HEP by phosphonoacetaldehyde reductase, utilizing NADH as a cofactor. Finally, MpnS catalyzed the oxidative conversion of 2-HEP to Mpn through an oxygen-dependent reaction mechanism.

To select suitable enzymes for this cascade, we screened candidate enzymes with analogous functions from diverse microbial sources using KEGG and NCBI databases, supplemented by literature mining. To overcome thermodynamic equilibrium barrier, the PEP mutase reaction was coupled with an irreversible downstream step, namely the decarboxylation of PnPy in this case. We selected PEP mutase (AepX) and phosphonopyruvate decarboxylase (AepY) from *Bacteroides fragilis* [16], both of which were successfully overexpressed in *E. coli* BL21(DE3). Although PEP mutase from *T. pyriformis* (PepM) and phosphonopyruvate decarboxylase (Fom2) from *Streptomyces wedmonrensis* were also evaluated, this combination ultimately did not meet expectations. This result suggested that Fom2 was inactive under the in vitro conditions tested. We assessed phosphonoacetaldehyde reductases from *Streptomyces monomycini* (AlpJ), *S. wedmorensis* (FomC), and *N.maritimus* (Pdh). Despite extensive efforts, FomC and Pdh were predominantly expressed as inclusion bodies in *E. coli* (Fig. S1), prompting the selection of soluble AlpJ for subsequent studies. Finally, methylphosphonate synthase (MpnS) from *N. maritimus* was confirmed to be soluble by SDS-PAGE analysis. Collectively, four enzymes (AepX, AepY, AlpJ, and MpnS) that exhibited both soluble expression and enzymatic activity were ultimately selected (Table 1). The purification of the four enzymes was shown in Fig. 2a.

Construction of in vitro multi-enzyme cascade

To further verify the feasibility of the selected enzymes for Mpn production, we reconstituted the biocatalytic cascade in vitro using purified enzymes and monitored phosphonate intermediates. To circumvent the

Table 1 The information on enzymes for cascade biocatalysis in this study

Enzyme	Source	Reaction	NCBI accession numbers
Phosphoenolpyruvate phosphomutase	*Bacteroides fragilis*	Phosphoenolpyruvate ⇆ 3-Phosphonopyruvate	AF285774
Phosphonopyruvate decarboxylase	*Bacteroides fragilis*	3-Phosphonopyruvate → Phosphonoacetaldehyde + CO_2	AF285774
Phosphonoacetaldehyde reductase	*Streptomyces monomycini*	Phosphonoacetaldehyde + NADH → 2-Hydroxyethylphosphonate + NAD^+	NZ_KL571064
Methylphosphonate synthase	*Nitrosopumilus maritimus*	2-Hydroxyethylphosphonate + O_2 → Methylphosphonate + HCO_3^-	CP000866

thermodynamic equilibrium limitation of PEP mutase ($\Delta G'^{\circ}$ = +17.9 kJ/mol, eQuilibrator database), AepX and AepY were co-incubated to drive the conversion of PEP to PnAA. In vitro reactions were analyzed by ^{31}P NMR spectroscopy (500 MHz, D_2O). After 16 h at 30 °C, a distinct signal at δ 8.8 ppm confirmed the accumulation of PnAA, demonstrating successful conversion of PEP (δ – 1.0 ppm) by the AepX and AepY (Fig. 2b). Subsequent addition of AlpJ and NADH generated a new resonance at δ 18.0 ppm, matching the chemical shift of authentic 2-HEP. Finally, the introduction of MpnS and O_2 resulted in the appearance of a signal at δ 21.5 ppm, corresponding to Mpn (Fig. 2b). Because ^{31}P NMR chemical shifts of phosphonates were affected by pH, minor observed differences were considered negligible (Fig. S2) [16]. The identities of intermediates and Mpn were further confirmed by LC-MS (Fig. S3). To further confirm the process and conversion rate of the pathway in vitro, purified enzymes (AepX, AepY, AlpJ, and MpnS) were combined at a molar rate of 2:2:1:2 with 10 mM PEP in 1 mL reaction system to produce Mpn. Based on ^{31}P NMR analysis, the change of intermediates during the reaction over time were detected. The reaction process curve showed that

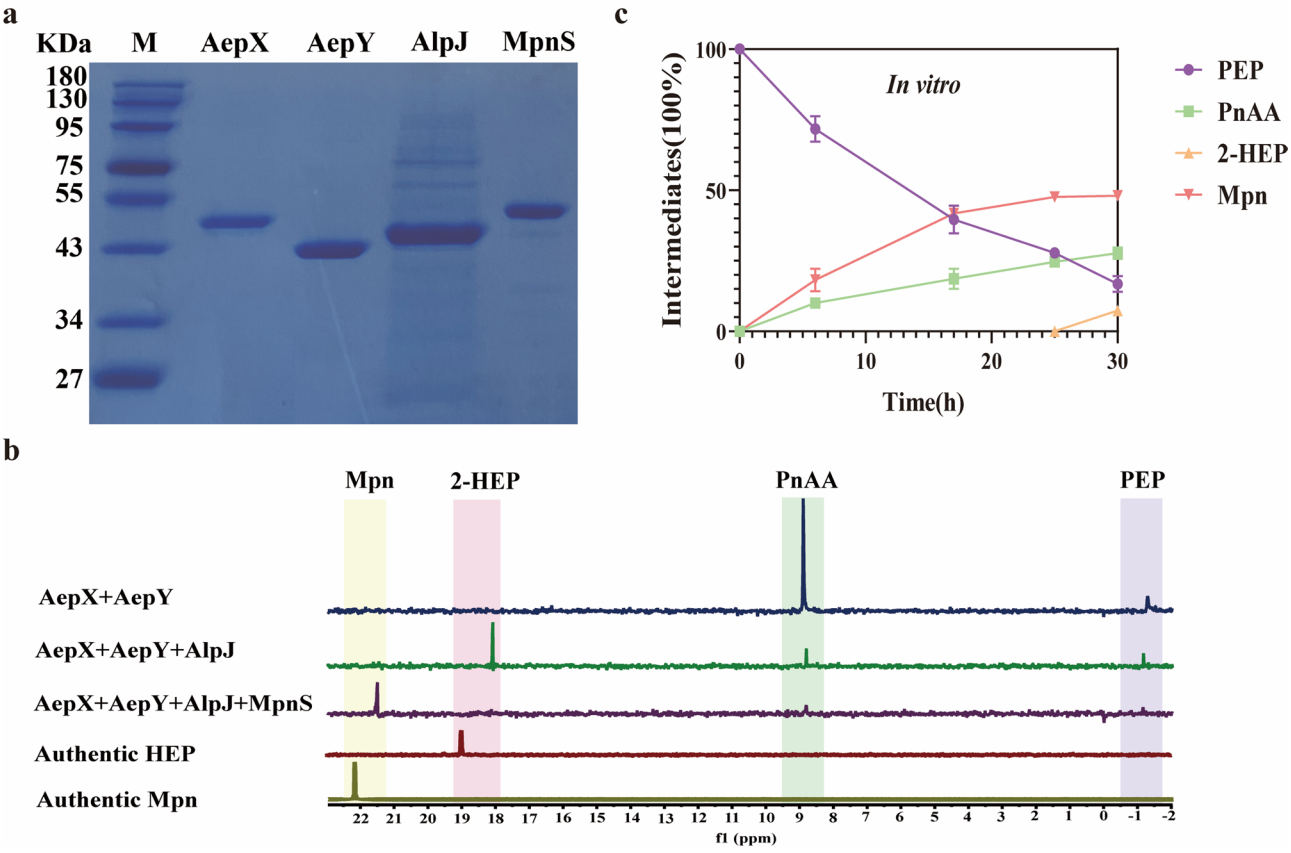

Fig. 2 **a** SDS-PAGE analysis of production and purification for four enzymes. AepX (48.9 kDa), AepY (41.2 kDa), AlpJ (41.9 kDa) and MpnS (52.1 kDa). **b** ^{31}P NMR analysis of intermediates for in vitro reaction. Each assay mixture included 20 μM of each enzyme. **c** The time course of in vitro reaction from PEP to Mpn and the reaction mixture had 10 μM of AepX, AepY and MpnS and 5 μM of AlpJ. Error bars present standard deviations of three biological replicates. The reactions were performed in 50 mM HEPES (pH 7.5), 10 mM PEP, 5 mM $MgCl_2$, 1.5 mM TPP, 5 mM NADH, 40 μM Fe (II)$(NH_4)_2$ $(SO_4)_2$

small intermediates PnAA and 2-HEP were accumulated and yielding Mpn with a 48% conversion at 30 h (Fig. 2c).

To further enhance the production of Mpn, the in vitro system was systematically optimized. The reaction time was set at 16 h. The effects of substrate (PEP) and NADH concentrations were first investigated to determine the optimum PEP/NADH ratio for the in vitro system (Fig. 3). The Mpn concentration increased as the PEP concentration increased from 1 to 5 mM and then gradually decreased upon further increase of the PEP concentration (Fig. 3a). Thus, the optimal concentration of PEP was 5 mM. Slight turbidity observed in reaction systems containing 10 mM and 15 mM PEP indicated that elevated PEP concentrations could inhibit enzyme activity, thereby reducing Mpn yield. Next, when 5 mM PEP was used, the NADH concentration was varied from 0.5 to 6 mM (Fig. 3b). The results indicated that Mpn production increased with increasing NADH concentration, reaching a maximum at 5 mM NADH. Therefore, we determined that the optimal ratio of substrate to NADH was around 1:1, which was consistent with theoretical NADH consumption in the reconstituted pathway (Fig. 1c). When more than 5mM $MgCl_2$ was used, no further increase in Mpn concentration was observed (Fig. 3c). Therefore, the optimal concentration of $MgCl_2$ was 5 mM. The concentration of TPP was further optimized using the predetermined optimal concentrations of PEP, NADH and $MgCl_2$ (5 mM each), yielding an optimal TPP concentration of 1.5 mM (Fig. 3d). Finally, the influence of enzyme concentration was investigated under optimal PEP (5 mM), NADH (5 mM), $MgCl_2$ (5 mM) and TPP (1.5 mM) condition. To determine the influence of each enzyme on the in vitro system, only one enzyme level was varied at a time by fixing the other three enzyme levels (10 μM). The results showed that each enzyme had varying effects on Mpn production. AepX exhibited saturation kinetics, with optimal activity observed at 5 μM, higher concentrations did not enhance the production of Mpn (Fig. 3e). In contrast, AepY required 10 μM for maximal activity (Fig. 3f). In contrast to AepX and AepY, varying the concentrations of AlpJ and MpnS over a range of 1 to 12 μM had a significant fluctuating impact on Mpn production in vitro. Mpn production reached a peak when AlpJ and MpnS concentrations were 10 μM, respectively (Fig. 3g-h). Based on these results, the optimal molar ratio of AepX: AepY: AlpJ: MpnS was determined to be 1:2:2:2. One such optimized synthetic unit (5 μM of AepX, 10 μM of AepY, AlpJ, MpnS) could produce 3.8 mM Mpn in 16 h with 76% molar conversion which corresponded to the result at 5 μM in Fig. 3e. This represented an approximately 1.5- fold increase in conversion yield compared to the initial, unbalanced enzyme ratio (2:2:1:2, Fig. 2b). In addition, we measured the rate of Mpn synthesis during the initial 5 h reaction phase across varying numbers of synthetic units (ranging from 1 to 5 optimized synthetic units) in 1mL in vitro system. Consequently, the addition of multiple synthetic units could increase the Mpn production efficiency, reaching up to 246.1μM Mpn/h with 5 optimized synthetic units (Fig. 3i).

Whole cells catalytic synthesis of Mpn from PEP

Based on the optimized in vitro system, recombinant *E. coli* strains co-expressing all four enzymes were engineered to serve as whole-cell biocatalysts for Mpn production. The enzyme concentration ratio was a key factor affecting the yield of Mpn in vitro. Therefore, to balance the expression levels of multiple enzymes in *E. coli*, a dual-plasmid system with different copy numbers (pRSFDuet: 100, pETDuet: 40, and pCDFDuet: 20) and two multiple cloning sites (MCSs) was employed to construct the recombinant strains. The four enzymes were distributed across two plasmids: one plasmid harboring AepX and AepY, and the other harboring AlpJ and MpnS. This strategy resulted in the construction of six distinct plasmid combinations (Table S1). Finally, six recombinant *E. coli* cells (E1-E6) were obtained (Fig. 4a). The catalytic capabilities of six recombinant strains were then evaluated using 20 mM PEP as the substrate, revealing variations in Mpn productivity. Strain E6 exhibited the highest production of Mpn (7.19 mM) after 16 h at 30℃. Strains E1, E2, and E5 produced Mpn at moderate levels (3.2 to 3.8 mM). E3 and E4 strains produced less than 2 mM Mpn (Fig. 4b). SDS-PAGE analysis confirmed distinct differences in enzyme expression profiles among the six recombinant strains (Fig. S3). Strain E6 exhibited high expression levels of all four enzymes, whereas E3 and E4 showed unbalanced expression patterns, correlating with their respective Mpn production levels. Specifically, the pRSFDuet, pETDuet, and pCDFDuet plasmids represent high, medium, and low levels of gene expression, respectively. The E6 strain, harboring the pCDFDuet-*aepX-aepY* and pETDuet-*alpJ-mpnS* plasmids, demonstrated the highest Mpn production. This indicated that this specific plasmid pairing facilitated coordinated reactions of the four enzymes, thereby enhancing Mpn biosynthesis. Compared to the wild-type strain, E6 exhibited reductions in growth rate and maximum OD600 (Fig. S6), indicating a measurable metabolic burden associated with heterologous plasmid maintenance and protein expression. Nevertheless, strain E6 maintained stable growth capability.

The in vivo system achieved a molar conversion yield of 35.95% (from 20 mM). To investigate potential intermediates accumulation and substrate retention, we conducted ^{31}P NMR analysis. ^{31}P NMR analysis revealed that most PEP was converted to an unidentified compound exhibiting a chemical shift at approximately 2.5 ppm, with minimal flux toward Mpn synthesis. Notably, no

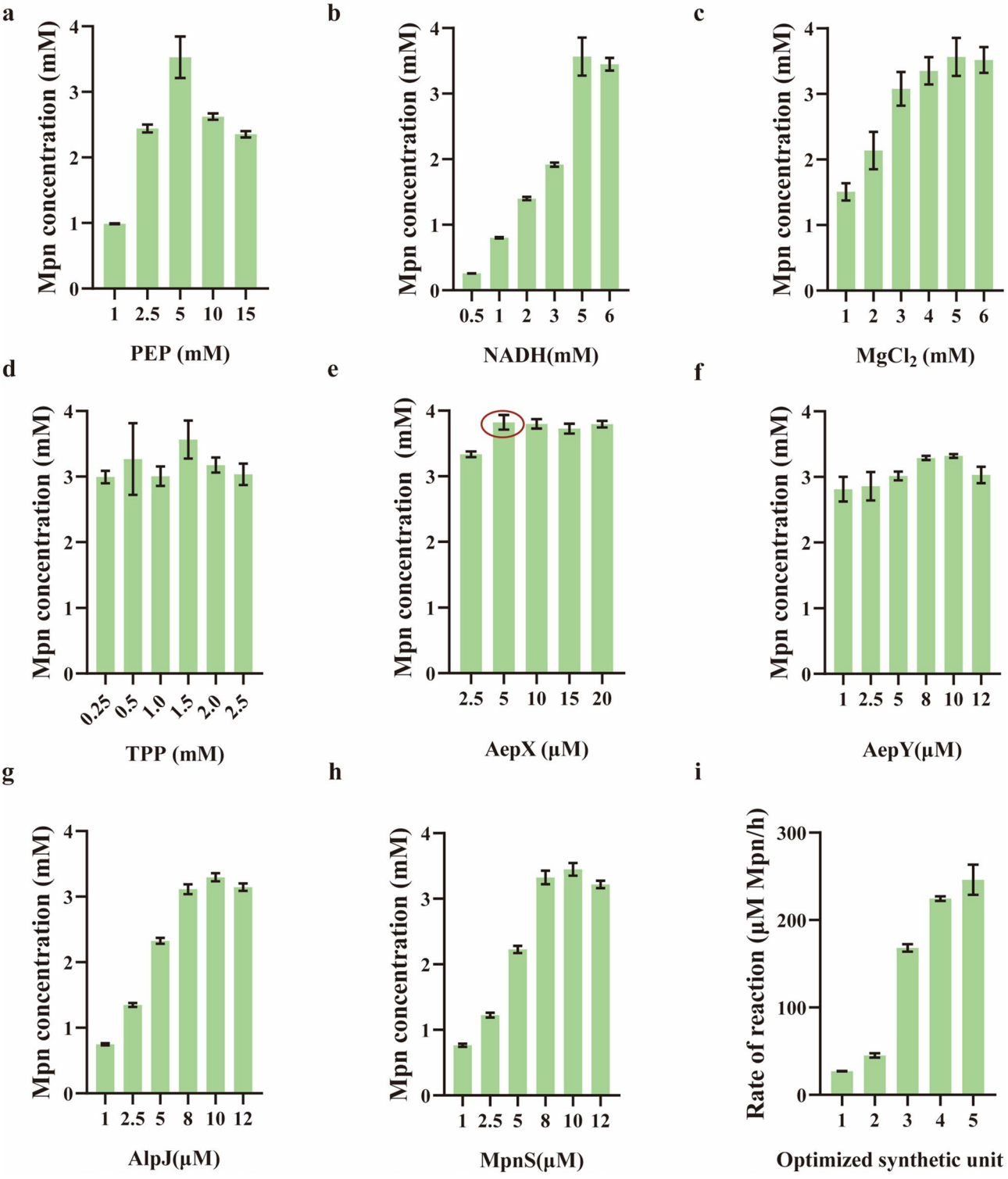

Fig. 3 Optimization of in vitro reaction conditions for the production of Mpn from PEP. **a** Substrate PEP. **b** Cofactor NADH. **c** MgCl2. **d** TPP. **e** AepX. **f** AepY. **g** AlpJ. **h** MpnS. **i** The effects of increased synthetic units to Mpn production and one synthetic unit has 5 μM AepX, 10 μM of AepY, AlpJ and MpnS. The reaction conditions were: a-d included 10 μM of each enzyme; **e**-**i** included 5 mM PEP, 5 mM $MgCl_2$, 1.5 mM TPP, 5 mM NADH, and varying concentrations of each enzyme. The circled point represented the highest Mpn yield. All the experiments were performed in triplicate, and data are presented as mean ± SD (standard deviation)

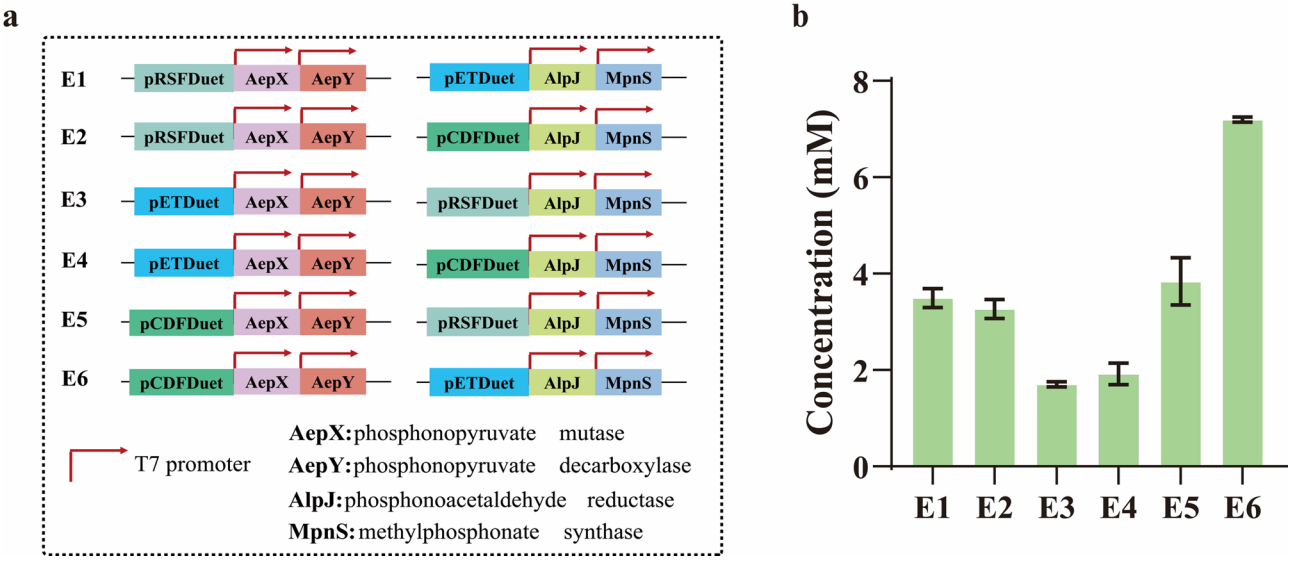

Fig. 4 **a** Construction of *E. coli* recombinants co-expression four enzymes. **b** The biotransformation activity of recombinants. All the experiments were performed in triplicate, and data are presented as mean ± SD

accumulation of intermediates was detected throughout the process. Comparison with the control results suggested that this phenomenon was from host interference (Fig. S7).

Discussion

To date, the synthesis of Mpn predominantly relies on chemical methods, and research on Mpn biosynthesis has primarily focused on the catalytic mechanism of MpnS [26, 27]. Notably, a dearth of studies exists concerning the practical application of the complete Mpn biosynthetic pathway. In this study, the Mpn biosynthetic pathway was reconstituted through a biocatalytic cascade for the first time. Through the screening of enzymes from diverse microorganisms and the characterization of reaction intermediates, we successfully demonstrated the biosynthesis of Mpn. For the in vitro synthesis, the Mpn production was improved following the optimization of reaction conditions. Cheng et al. also found that enzymatic process optimization could apparently enhance isoprene production [28]. In the whole-cell catalytic synthesis, the modulation of plasmid copy numbers was shown to influence the balance of multi-enzyme expression [17], consequently affecting Mpn production. Both in vitro and in vivo synthesis underscored the critical role of multi-enzyme coordination in Mpn production. Compared to the in vivo biosynthesis system, the in vitro enzymatic system achieved higher conversion efficiency in this investigation. However, the in vitro system has some limitations. Firstly, the overexpression and purification of multiple enzymes impose additional labor and economic costs. Secondly, the requirement for expensive cofactors undermines economic feasibility, hampering large-scale production. In contrast, the in vivo system could bypass these limitations and shows potential for scalable biosynthesis of Mpn, though its current performance requires further optimization.

The in vivo synthesis system developed in this study exhibited a low conversion rate, accompanied by significant byproduct accumulation. We hypothesized that PEP, a key intermediate in glycolysis [29], was predominantly metabolized through endogenous metabolic pathways rather than being channeled into the heterologous biosynthetic pathway. This metabolic competition ultimately favored bacterial growth over the synthesis of the target compound. These findings highlight the critical need to optimize the interplay between the heterologous synthesis pathway and the endogenous metabolism of *E. coli* to enhance in vivo production efficiency. Therefore, addressing this bottleneck remains a critical research priority in our future work.

Metabolic engineering represents a promising strategy for redirecting metabolic flux towards the synthesis of target compounds in engineered strains [30]. Genetic editing tools can be employed to rewire the host's metabolic network, thereby enhancing carbon flux from substrate glucose to PEP and ultimately boosting Mpn production. Xue et al. enhanced the carbon flux through the shikimate pathway by inhibiting a competitive pathway to promote PEP acquisition [31]. Furthermore, the exploration of cheaper and more sustainable substrates will improve the economic feasibility of Mpn biosynthesis [32].

Conclusions

In this study, we developed a biocatalytic cascade for the production of Mpn from PEP. Initially, through systematic enzyme screening, we selected four enzymes essential for converting PEP to Mpn and successfully reconstituted the Mpn biosynthetic pathway in vitro. Subsequently, we optimized the in vitro multi-enzyme reaction conditions and obtained an Mpn yield of 76%, representing a 1.5-fold increase over the pre-optimization. Building on the in vitro results, recombinant *E. coli* strains co-expressing the cascade enzymes were engineered as whole-cell biocatalysts. The synthetic potential of strains with varying plasmid combinations was confirmed. The optimal strain produced 7.19 mM Mpn, corresponding to a molar conversion rate of 35.95%. This work established a proof-of-concept biocatalytic platform for Mpn production. However, the current system was limited by its dependence on expensive cofactors in vitro and low conversion efficiency in vivo. Future efforts will focus on metabolic engineering and cost reduction to enable practical applications.

Materials and methods

Chemicals and strains

PEP, IPTG, ampicillin, kanamycin, streptomycin, thiamine diphosphate (TPP), 4- (2-hydro-xyethyl) -1-piperazineethanesulfonic acid (HEPES, pH 7.5), imidazole and Luria-Bertani (LB) medium were from Macklin (Shanghai, China). Taq DNA polymerase was from Takara (Beijing, China). DNA Assembly Cloning Kit was from NEB (Beijing, China). The Plasmid isolation kit was from Tiangen (Beijing, China).

Bacterial strains and plasmids used in this study were listed in Table S1. *E. coli* BL21(DE3) and *E. coli* DH5α were used for recombinant protein expression and cloning, respectively. All genes used in this study were synthesized and gene sequences were optimized by Tsingke (Beijing, China). Antibiotics were added at a final concentration of 50 μg/mL, 100 μg/mL, and 100 μg/mL for kanamycin, ampicillin, and streptomycin, respectively.

Enzyme expression and purification

For enzyme selection, we primarily utilized KEGG and NCBI databases to screen enzymes with the desired functions, selecting those exhibiting both soluble expression and enzymatic activity. The pET28a-*aepX*, pET28a-*aepY*, pET15b-*alpJ*, and pET28a-*mpnS* recombinant plasmids were transformed into *E. coli* BL21 (DE3) to express four proteins, respectively. The *E. coli* BL21 (DE3) containing the protein expression plasmids was cultivated in the 500 mL LB medium with kanamycin or ampicillin at 37℃. When the OD600 reached 0.6–0.8, 0.1 mM IPTG (a final concentration) was added and the cultivation temperature was decreased to 16℃ for recombinant protein expression. After growth for 16 h, cells were harvested by centrifugation at 4℃, washed twice, and resuspended by 50 mM HEPES buffer (pH 7.5). The suspension was lysed by sonication (at 400 W with 4 s pulses and 4 s intervals between each cycle) for 20 min in an ice bath. After centrifugation at 4℃ and 12,000 rpm for 30 min, the supernatant was further purified by a 2 mL Nickel-Nitrilotriacetic Acid (Ni-NTA) column. The Nickel Column was washed with 10 mL water and 10 mL binding buffer (50 mM HEPES at pH 7.5 with 20 mM imidazole and 300 mM NaCl) before being used to ensure that the column was equilibrated, and then the protein harboring 6×His tag was able to bind Nickel column specifically. Unbound and nonspecific proteins were washed out with 20 mL washing buffer (50 mM HEPES at pH 7.5 with 20 mM or 60 mM imidazole and 300 mM NaCl). The 10 mL elution buffer (50 mM HEPES at pH 7.5 with 250 mM imidazole and 300 mM NaCl) was used to wash specific proteins. Finally, the column was re-equilibrated with a buffer. The protein concentrations were measured using the BCA method and the BSA standard was used for plotting the calibration curve. The purified proteins were stored at -80℃.

The assay of intermediates

The reaction mixture was carried out in 1mL 50 mM HEPES (pH 7.5) containing 10 mM PEP, 5 mM Mg^{2+}, 1.5 mM TPP, and 20 μM each of AepX and AepY, respectively. Subsequently, 5 mM NADH and 20 μM AlpJ were mixed to prepare 2-HEP in the above reaction solution which had been boiled to deactivate AepX and AepY. Finally, the 20 μM final enzyme MpnS and 40 μM Fe^{2+} were added to produce Mpn after the AlpJ was activated. Additionally, the final reaction solution was saturated with O_2 on ice to increase the amount of dissolved O_2. The above reaction mixtures were incubated in 30℃ for 16 h to ensure that the reaction was complete. These three products PnAA, 2-HEP and Mpn were determined by ^{31}P NMR and LC-MS. The Mpn one pot reaction contained 10 mM PEP, 5 mM $MgCl_2$, 1.5 mM TPP, 5 mM NADH, 40 μM Fe (II)$(NH_4)_2$ $(SO_4)_2$, and four enzymes (AepX: 10 μM, AepY: 10 μM, AlpJ: 5 μM and MpnS: 10 μM).

D_2O (20% v/v) was added to all reaction samples as a lock solvent and then transferred to NMR tubes. All NMR spectra were recorded on a JEOL JNM-ECZR 500 MHz spectrometer equipped with a 5 mm FG/ROHFX probe at 25℃. LC-MS analysis was performed on a Thermo Scientific UltiMate 3000 system equipped with a C18 column (Accucore™ aQ 100 × 2.1 mm 2.6 μm). The column temperature was 25℃. The liquid chromatography gradient was: 0–1 min, 98% B; 1–4 min, 98% B-80% B; 4–8 min 80% B-50% B; 8–8.1 min, 50% B-98% B; 8.1–10 min, 98% B at a flow rate of 0.4 mL/min. Solvent A: Acetonitrile

(ACN); Solvent B: ultrapure water added 0.1% formic acid. The mass spectrometry instrument was set as follows: Ion source type = H-ESI, Spray voltage: Negative ion (V) = 3200, Sheath gas = 40, Aux gas = 10, Ion transfer tube temperature = 320 ℃. Mpn was quantified using the LC-MS method and the scan mode was Selected Reaction Monitoring (SRM). The mother mass was set to *m/z* 95.122 and the product mass was set to *m/z* 79.22. The sample area was converted to Mpn concentration by comparing with a standard curve plotted with a set of known concentrations of Mpn standard samples. The MS scan mode of intermediate was Full scan.

Optimization of the in vitro reaction conditions

PEP, NADH, $MgCl_2$, and TPP concentration were optimized in a 500 μL reaction system containing 50 mM HEPES buffer (pH 7.5) and 10 μM of each enzyme, incubated at 30℃ for 16 h. The PEP concentration gradient was first set from 1 to 15 mM in reaction conditions containing 5 mM $MgCl_2$, 1.5 mM TPP, and 10 mM NADH. After determining the optimal PEP concentration, the concentration of NADH was changed from 0.5 to 6 mM in 5 mM $MgCl_2$ and 1.5 mM TPP reaction conditions. The concentration of $MgCl_2$ varied from 1 to 6 mM in reaction mixture containing optimal PEP and NADH and 1.5 mM TPP. The TPP concentration was subsequently changed from 0.25 to 2.5 mM in reaction buffer containing optimal PEP, NADH and $MgCl_2$. After the concentration of PEP, NADH, $MgCl_2$ and TPP were determined, enzyme ratio was further optimized. The concentration of enzyme varied from 0 to 20 μM in optimal PEP, $MgCl_2$, cofactor NADH, and TPP conditions. When the concentration of one enzyme was varied, the concentrations of the other three enzymes were maintained 10 μM.

Construction of the recombinant *E. coli* strain

For *E. coli* E1-E6, the plasmid pET28a-*aepX*, pET28a-*aepY*, pET15b-*alpJ* and pET28a-*mpnS* were used as template for genes *aepX*, *aepY*, *alpJ* and *mpnS* amplification by PCR using specificity primers (Table S2). The plasmid pRSFDuet, pETDuet, and pCDFDuet were also linearized by PCR. Genes and linearized plasmids were ligated by Gibson Assembly to form six recombinant plasmids (pRSFDuet-*aepX-aepY*/ pRSFDuet-*alpJ-mpnS*, pETDuet-*alpJ-mpnS*/ pETDuet-*aepX-aepY*, and pCDFDuet-*aepX-aepY*/ pCDFDuet-*alpJ-mpnS*). These recombinant plasmids were transformed into *E. coli* BL21 (DE3) to construct six recombinants in pairwise combinations. When the OD600 reached 0.6–0.8, 0.4 mM IPTG (a final concentration) was added and the cultivation temperature was decreased to 25℃ for protein expression. After growth for 16 h, recombinant cells were harvested as whole-cell biocatalysts for Mpn production. Biotransformation of PEP to Mpn was performed at 30℃ and 200 rpm for 16 h with 2 mL of 50 mM HEPES buffer (pH 7.5) containing 20 mM PEP, 5 mM $MgCl_2$, 1.5 mM TPP, and 50 mg/mL wet cell weight of recombinant *E. coli*.

Abbreviations

PEP	Phosphoenolpyruvate
PnPy	Phosphonopyruvate
PnAA	Phosphonoacetaldehyde
2-HEP	2-hydroxyethylphosphonate
Mpn	Methylphosphonate
AepX	Phosphoenolpyruvate phosphomutase
AepY	Phosphonopyruvate decarboxylase
AlpJ	Phosphonoacetaldehyde reductase
MpnS	Methylphosphonate synthase
SDS-PAGE	Sodium dodecyl sulfate polyacrylamide gel electrophoresis
IPTG	Isopropyl β-D-thiogalactoside
LC-MS	Liquid Chromatograph Mass Spectrometer
^{31}P NMR	^{31}P Nuclear Magnetic Resonance
HEPES	4-(2-hydro-xyethyl)-1-piperazineethanesulfonic acid
TPP	Thiamine diphosphate

Supplementary Information

The online version contains supplementary material available at https://doi.org/10.1186/s12934-025-02858-y.

Supplementary Material 1.

Acknowledgements

No applicable.

Author contributions

Qi Zhang: methodology, formal analysis, and writing original draft. Bobo Wang, Cong Wang and Renyuan Zhao: methodology, investigation, and validation. Yiming Zhang and Zhisheng Yu: methodology, supervision, revision, and conceptualization.

Funding

The present study was supported by the National Natural Science Foundation of China (No. 42307181), and the Fundamental Research Funds for the Central Universities (No. E0E48965×2), for the realization of this investigation.

Data availability

No datasets were generated or analysed during the current study.

Declarations

Ethics approval and consent to participate

No applicable.

Consent for publication

No applicable.

Competing interests

The authors declare no competing interests.

Received: 3 June 2025 / Accepted: 13 October 2025
Published online: 14 November 2025

References

1. Horsman G, Zechel D. Phosphonate biochemistry. Chem Rev. 2016;117:5704–83.
2. Atanasov V, Lee A, Park E, Maurya S, Baca E, Fujimoto C, Hibbs M, Matanović I, Kerres J, Kim Y. Synergistically integrated phosphonated Poly (pentafluorostyrene) for fuel cells. Nat Mater. 2021;20:1–8.

3. Krečmerová M, Majer P, Rais R, Slusher B. Phosphonates and phosphonate prodrugs in medicinal chemistry: past successes and future prospects. Front Chem. 2022;10:889737.
4. Wei Y, Qiu G, Lei B, Qin L, Lu Y, Zhu G, Gao Q, Huang Q, Qian G, Liao P, et al. Oral delivery of Propofol with methoxymethylphosphonic acid as the delivery vehicle. J Med Chem. 2017;60:8580–90.
5. Karl D, Beversdorf L, Orkman K, Church M, Martinez A, Delong E. Aerobic production of methane in the sea. Nat Geosci. 2008;1:437–78.
6. Silva V, Santos Y, Hellinger R, Mansour S, Delaune A, Legros J, Zinoviev S, Nogueira E, Orth E. Organophosphorus chemical security from a peaceful perspective: sustainable practices in synthesis, decontamination and detection. Green Chem. 2021;24.
7. Ma XT, Xu Q, Li H, Su CL, Yu L, Zhang X, Cao HG, Han LB. Alcohol-based Michaelis-Arbuzov reaction: an efficient and environmentally-benign method for C-P(O) bond formation. Green Chem. 2018;20:3408–13.
8. Jansa P, Holy A, Dracinsky M, Baszczynski O, Cesnek M, Janeba Z. Efficient and 'green' microwave-assisted synthesis of haloalkylphosphonates via the Michaelis-Arbuzov reaction. Green Chem. 2011;13:882–8.
9. Demmer CS, Krogsgaard-Larsen N, Bunch L. Review on modern advances of chemical methods for the introduction of a phosphonic acid group. Chem Rev. 2011;111:7981–8006.
10. Sevrain CM, Berchel M, Couthon H, Jaffrès PA. Phosphonic acid: Preparation and applications. Beilstein J Org Chem. 2017;13:2186–213.
11. Bell E, Finnigan W, France S, Green A, Hayes M, Hepworth L, Lovelock S, Niikura H, Osuna S, Romero E, et al. Biocatal Nat Rev Methods Primers. 2021;46:1–21.
12. Yi J, Li Z. Artificial multi-enzyme cascades for natural product synthesis. Curr Opin Biotechnol. 2022;78:102831.
13. Kuska J, O'Reilly E. Engineered biosynthetic pathways and biocatalytic cascades for sustainable synthesis. Curr Opin Chem Biol. 2020;58:146–54.
14. Huffman M, Fryszkowska A, Alvizo O, Borra M, Campos K, Canada K, Devine P, Duan D, Forstater J, Grosser S, et al. Design of an *in vitro* biocatalytic cascade for the manufacture of Islatravir. Sci. 2019;366:1255–9.
15. Gao D, Song W, Liang G, Gao C, Liu H, Chen X, Liu J. Efficient production of L-Homophenylalanine by enzymatic-chemical cascade catalysis. Angew Chem Int Ed. 2022;61:e202207077.
16. Otte K, Kittelberger J, Kirtz M, Nestl B, Hauer B. Whole-cell one-pot biosynthesis of Azelaic acid. ChemCatChem. 2014;6:1003–9.
17. Zhao R, Huang S, Gao L, Zhang J. One-pot biocatalytic upgrading of lignin-derived phenol and catechol to Hydroxytyrosol. Green Chem. 2024;26:6180–9.
18. Zhou H, Wang B, Wang F, Yu X, Ma L, Li A, Reetz M. Chemo - and regioselective dihydroxylation of benzene to hydroquinone enabled by engineered cytochrome P450 monooxygenase. Angew Chem Int Ed. 2018;131:764–8.
19. Metcalf W, Griffin B, Cicchillo R, Gao J, Janga SC, Cooke H, Circello B, Evans B, Martens-Habbena W, Stahl D, Donk W. Synthesis of methylphosphonic acid by marine microbes: a source for methane in the aerobic ocean. Sci. 2012;337:1104–7.
20. Shiraishi T, Kuzuyama T. Biosynthetic pathways and enzymes involved in the production of phosphonic acid natural products. Biosci Biotechnol Biochem. 2021;85:42–52.
21. Blodgett J, Thomas P, Li G, Velasquez J, Donk W, Kelleher N, Metcalf W. Unusual transformations in the biosynthesis of the antibiotic phosphinothricin tripeptide. Nat Chem Biol. 2007;3:480–5.
22. Zhang Y, Chen L, Wilson J, Cui J, Roodhouse H, Kayrouz C, Pham T, Ju K-S. Valinophos reveals a new route in microbial phosphonate biosynthesis that is broadly conserved in nature. J Am Chem Soc. 2022;144:9938–48.
23. Chu LX, Luo XX, Zhu T, Cao YY, Zhang L, Deng Z, Gao JT. Harnessing phosphonate antibiotics Argolaphos biosynthesis enables a synthetic biology-based green synthesis of glyphosate. Nat Commun. 2022;13:1–16.
24. Ju KS, Gao J, Doroghazi J, Wang KK, Thibodeaux C, Li S, Metzger E, Fudala J, Su J, Zhang J, et al. Discovery of phosphonic acid natural products by mining the genomes of 10,000 actinomycetes. Proc Natl Acad Sci USA. 2015;112:12175–80.
25. Seidel H, Freeman S, Seto H, Knowles J. Phosphonate biosynthesis: isolation of the enzyme responsible for the formation of a carbon-phosphorus bond. Nat. 1988;335:457–8.
26. Wang B, Cao Z, Rovira C, Song J, Shaik S. Fenton-derived OH radicals enable the MPnS enzyme to convert 2-hydroxyethylphosphonate to methylphosphonate: insights from Ab initio QM/MM MD simulations. J Am Chem Soc. 2019;141.
27. Born D, Ulrich E, Ju KS, Peck S, Donk W, Drennan C. Structural basis for methylphosphonate biosynthesis. Sci. 2017;358:1336–9.
28. Cheng T, Liu H, Zou HB, Chen NN, Shi MX, Xie CX, Zhao G, Xian M. Enzymatic process optimization for the in vitro production of isoprene from mevalonate. Microb Cell Fact. 2017;16.
29. Fuentes E, Usgame K, Fierro A, López C. Enzymes of Glycolysis and the Pentose phosphate pathway as targets of oxidants: role of redox reactions on the carbohydrate catabolism. RBC. 2025;11:100049.
30. Wu ZK, Liang XQ, Li MK, Ma MY, Zheng QS, Li DF, An TY, Wang GL. Advances in the optimization of central carbon metabolism in metabolic engineering. Microb Cell Fact. 2023;22.
31. Xue BQ, Lu LY, Hu CY, Cheng YY, Wang XL, Zhang W, Wang T, Ren JD, Shen XL, Sun XX, et al. Metabolic engineering of *Escherichia coli* for efficient production of benzyl alcohol. Agric Food Chem. 2025;73:12374–82.
32. Fujiwara R, Noda S, Tanaka T, Kondo A. Metabolic engineering of *Escherichia coli* for Shikimate pathway derivative production from glucose-xylose co-substrate. Nat Commun. 2020;11.

Publisher's Note